Material Selection and Thermal Design for the Tracker Sidewalls of GLAST

Scott Keating, Stephen Ney, Eric Ponslet, Erik Swensen
10/27/2000

	Name:	Phone:	Signature:
Main Author:	Scott Keating	505.661.9020	
Approved:	Erik Swensen	505.661.4021	

Abstract

This report describes the material selection and thermal design for the tracker tower sidewalls of the Gamma-ray Large Area Space Telescope (GLAST). The tracker is comprised of 16 prismatic towers, each of which contains a stacked-tray arrangement of gamma-ray sensing and data acquisition components.

The tracker sidewalls form the outer shell of the towers and serve to provide support, containment and shielding, and alignment for the stacked trays. The sidewalls also provide an important function by serving as thermal conduits to evacuate heat from electrical components of the tracker trays. This report presents material options and summarizes the material selection and thermal design for the tracker sidewalls.

DESIGN ENGINEERING
ADVANCED COMPOSITE APPLICATIONS
ULTRA-STABLE PLATFORMS

110 EASTGATE DR.
LOS ALAMOS, NM 87544

PHONE 505 661•3000
FAX 505 662•5179
WWW.HYTECINC.COM

Revision Log

Rev.	Date	Author(s)	Summary of Revisions/Comments
Draft	May 18, 2000	Scott Keating	Draft for review

Table of Contents

1. Definitions

ACD	Anti-Coincidence Detector
CC	Carbon-carbon (composite)
GLAST	Gamma-ray Large Area Space Telescope
Gr-Ep	Graphite-Epoxy (composite)
S/W	Stiffness to weight ratio

2. Introduction

The GLAST science instrument (SI) is comprised of several principal components including the ACD, tracker, calorimeter, and structural grid. Figure 1 shows the current conceptual design for the GLAST SI.

The tracker detects gamma rays and contains electronics and physical elements to determine the path and intensity of the rays. The tracker is comprised of 16 prismatic towers, arranged in a 4 x 4 grid. In the current design, each tower consists of 19-stacked trays, held in position by post-tensioned cables during assembly and by flat panel sidewalls for handling, transport and flight. The sidewalls also serve as thermal conduits to remove heat from the tracker towers during operation of the SI. In this document, we describe material selection for the tracker sidewalls based on thermal analyses, stiffness, and material radiation length.

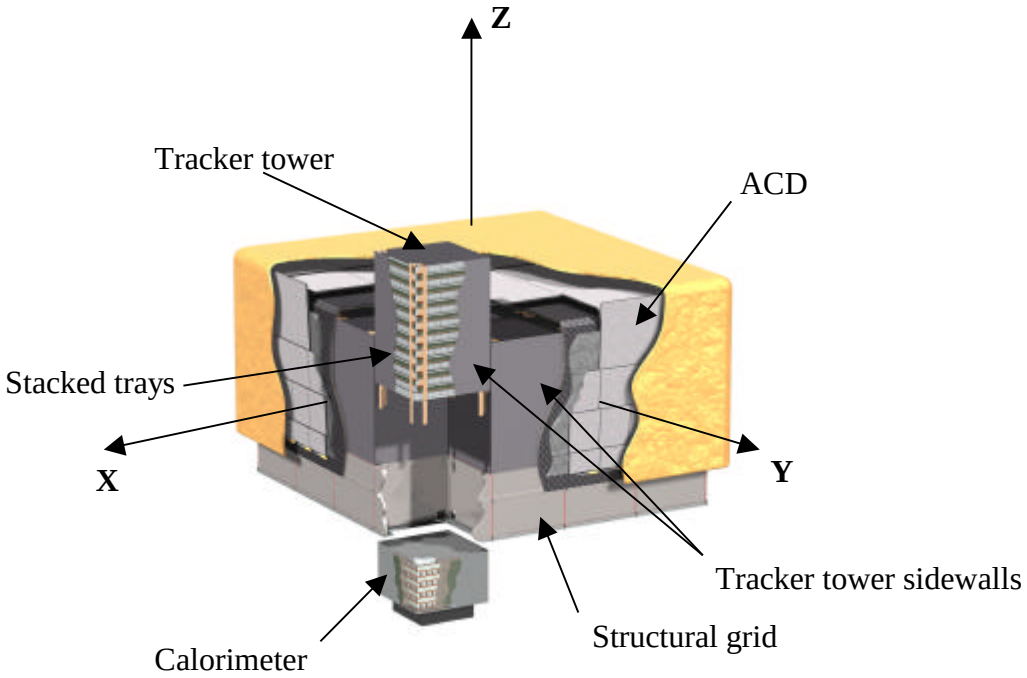

Figure 1: Current conceptual design for the GLAST SI.

3. Sidewall Design Considerations

Overall tracker design requirements can be found in HTN-102050-0021[1]. This section describes primary material and design considerations for the tracker sidewalls.

For the tracker application, the primary design considerations are:

1. Geometric stability – the instrumented trays must remain aligned for all phases of the SI life. Thus, the sidewall material must then provide the necessary structural stiffness and stability under thermal loads to ensure alignment of the trays during the SI life.
2. Thermal performance – the tracker produces a significant amount of heat. Because the sidewalls serve as the primary conduits for tracker heat dissipation, their thermal performance is critical.
3. Minimization of inactive regions – the inter-tower spacing and wall thickness are designed to be as small as possible to minimize inactive regions. This will maximize tracker coverage while reducing tower structure-instrument interference and weight.
4. Material radiation length – materials with higher radiation lengths (RL) will produce fewer spurious events to be detected by the tracker. It is advantageous to keep the RL as high as possible.

4. Properties of Potential Sidewall Materials

Several materials are available for spaceflight applications – metals (e.g., aluminum and beryllium) and composites (e.g., graphite-epoxy and carbon-carbon) are common categories. Thermal conductivity and coefficients of expansion for representative metal and composite materials are given in Figure 2 and Figure 3, respectively. Stiffness-to-density ratios are given in Figure 4. Figure 5 shows radiation lengths for the various materials.

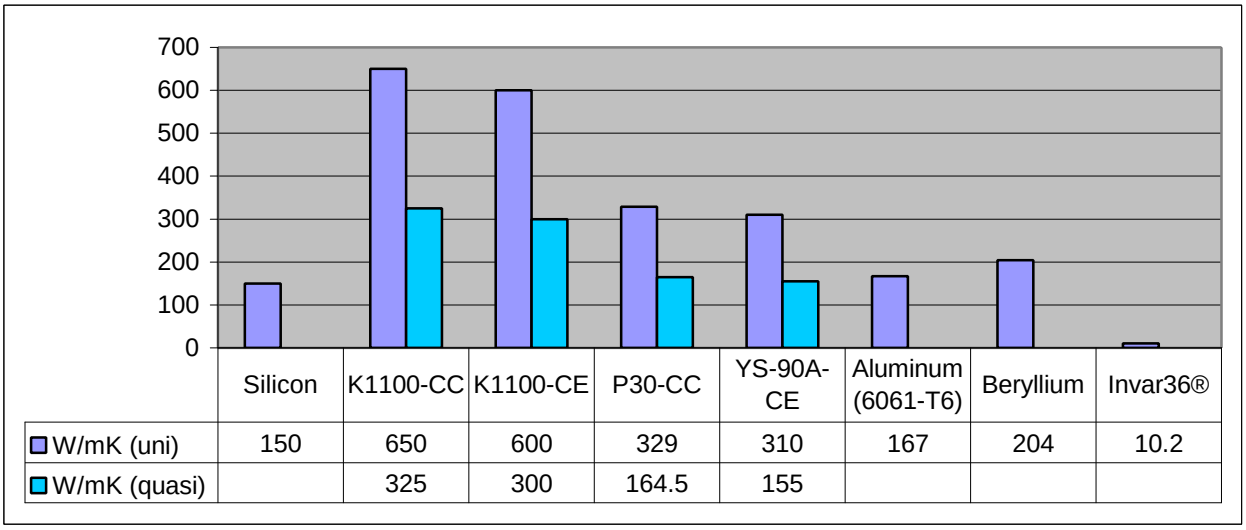

	Silicon	K1100-CC	K1100-CE	P30-CC	YS-90A-CE	Aluminum (6061-T6)	Beryllium	Invar36®
W/mK (uni)	150	650	600	329	310	167	204	10.2
W/mK (quasi)		325	300	164.5	155			

Figure 2: Thermal conductivity coefficients for various materials – unidirectional lamina and quasi-orthotropic values given for composites; units are in W/mK.

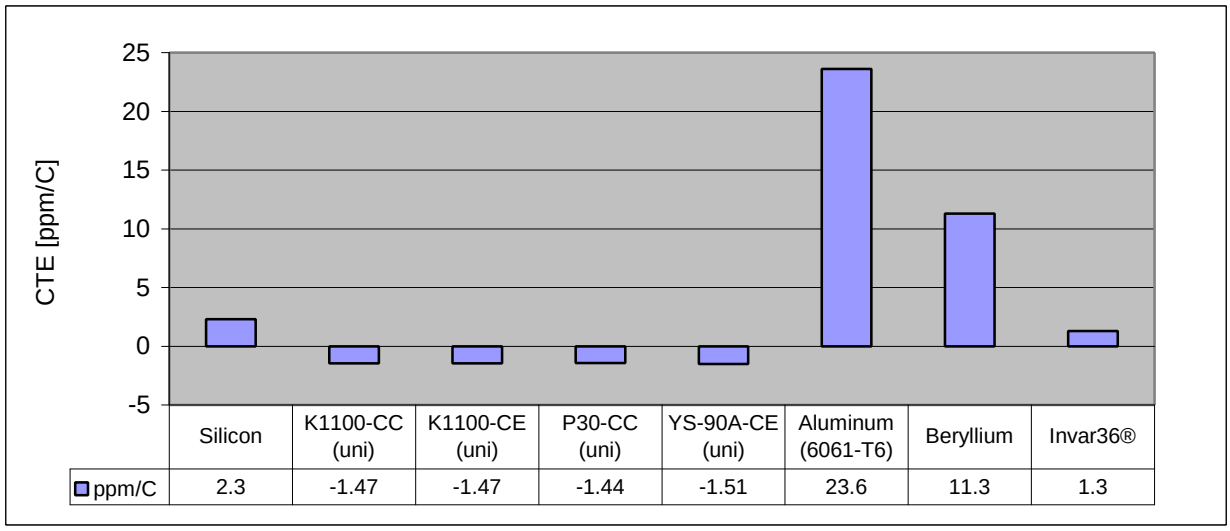

Figure 3: Coefficient of thermal expansion for various materials; units are in ppm/℃.

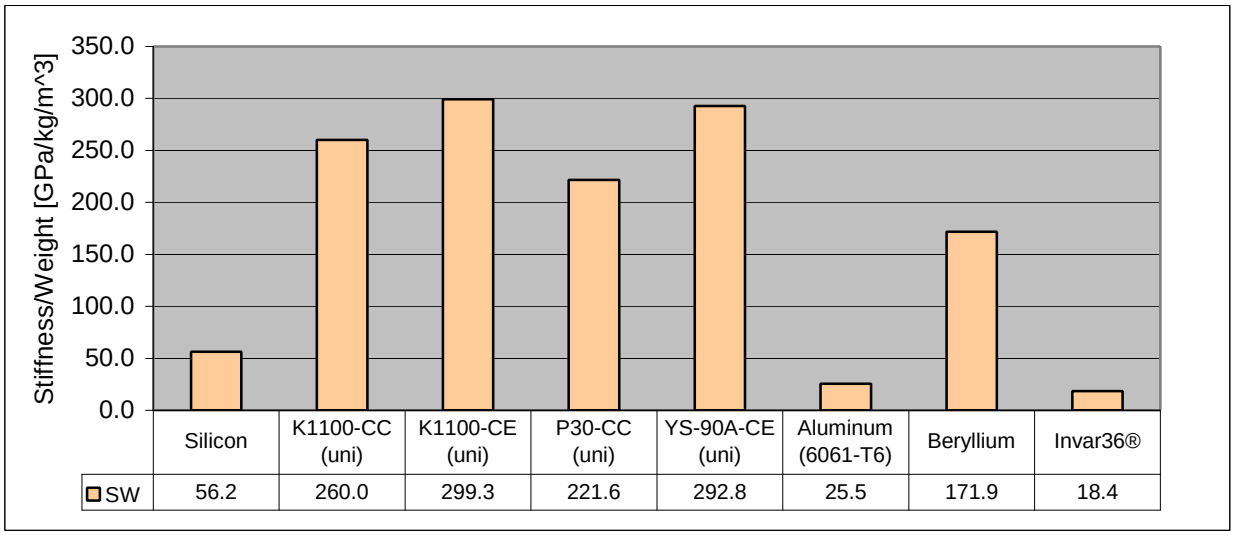

Figure 4: Stiffness to weight ratios for various materials; units are GPa/kg/m^3.

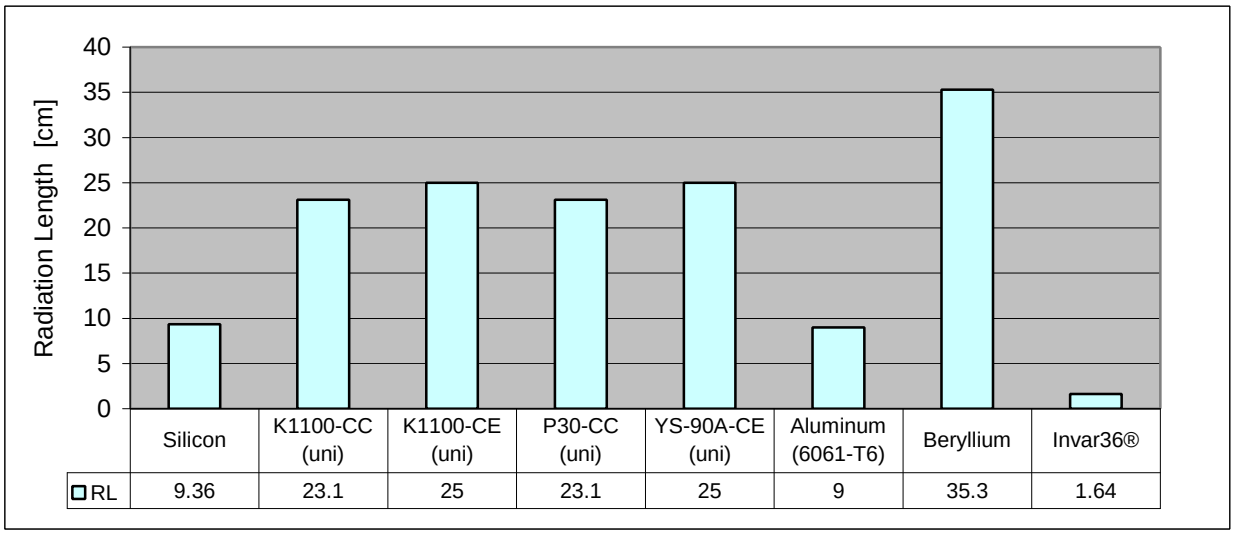

Figure 5: Radiation lengths for various materials; units are in cm.

5. Sidewall Material Selection

Based on the design considerations in Section 3, we review some candidate materials and select the best-suited materials for the sidewalls.

5.1 Thermal Conduction of Sidewall Material

Each tray produces approximately 0.9W of power [1]. A design requirement is that the tracker sidewall will transfer enough heat energy so that the top-to-bottom temperature differential of the tracker tower does not exceed 7ºC [1]. Additionally, the overall temperature of any individual tray should not exceed 25ºC [1].

For material selection purposes based on thermal performance, we start by conducting a 1-dimensional (1-D) heat conduction analysis. The equation for 1-D thermal conduction in a material of uniform cross-section, is

$$q_z = -k_z \frac{\partial T}{\partial z} A_c, \qquad (1)$$

where

q_z = power along the z-axis of the tracker tower sidewall

T = temperature

k_z = thermal conductivity

L = length of the sidewall

A_c = cross-sectional area of the sidewall (1.5mm X 392.5mm)

The 19 trays are alternately clocked at 0° and 90° such that every other tray, having two thermal bosses, connects thermally to opposing sidewalls (i.e., every other tray contributes a heat load to the same two opposing walls; the complementary trays connect thermally to the other two walls). If we make the assumption that 0.45W (1/2 of the tray power) is applied at 10 equally spaced locations, from the bottom to the top of each tower, then the power distribution is linear along the sidewall (~7.5W/m). Integrating Equation (1) yields a parabolic temperature distribution with a bottom to top temperature differential (in °C) of approximately

$$\Delta T = \frac{2450}{k_z}. \qquad (2)$$

From the materials shown in Figure 2, we can select several materials to analyze. Beryllium and aluminum are common spacecraft/SI materials, which have conduction coefficients of 204 and 167W/mK, respectively. These conduction values would yield a ΔT of 12.0°C for beryllium and 14.7°C for aluminum, which are outside of the specified design range. Other metals will produce similar or less desirable results.

Graphite-epoxy and carbon-carbon composites are also frequently used in space applications. Thermal conduction coefficients for composite laminates depend on fiber and matrix materials and lamina ply angles. 1-D thermal conduction values for composite laminae (single layer) can range from 350 to 600W/mK. These numbers are reduced for laminates (multi-layer) when ply angles are oriented to meet structural requirements. Figure 2 shows conduction values for both unidirectional and quasi-orthotropic composites, which bracket potential laminate layup values. Possible layups can yield 1-D laminate conduction values ranging from 150 to 450W/mK. In this range, we see that the estimated ΔT can be brought as low as 5.5°C, well within the design specification. From this simple analysis, we can conclude that carbon composites are likely the best materials for sidewall construction, based on thermal conduction requirements.

5.2 Carbon Fiber Selection

From figure 2, the four carbon composites shown have a substantial advantage over other more traditional materials with thermal conductivity. Figure 2 graphs the thermal conductivity in both the 0^o and 90^o directions for a single ply and multiple plies. K1100 carbon-carbon and cynate ester composites have the largest thermal conductance of the four carbon composites, making them the ideal fiber choice for the thermal part of the sidewall design. Unfortunately, K1100 is one of the most expensive fibers because of its high thermal conductivity. To use K1100 fibers would mean a large impact to program costs for the tracker towers.

The P30 fibers have a slightly higher thermal conductivity than the YS90A fibers when in the carbon-carbon state. Both are equally priced to one another, but the procurement time for the P30 C-C is longer than the YS90A CE. P30 C-C does have an impact on schedule for both the engineering model and the flight hardware. For the purposes of initial tests, both P30 C-C and YS90A CE sidewall test panels are to be tested structurally and thermally to determine final selection of material for sidewall panels.

5.3 Carbon Fiber/Ply Orientation

The mechanical and thermal properties of the carbon composites listed in table 2 through table 5 are from Conley for a single lamina ply. In order to determine the thermal properties of the entire sidewall laminate, the individual lamina properties must be defined from the fiber and resin matrix. Since the sidewall laminate consists of multiple plies orientated at different angles, a rotation of thermal properties back to the original coordinate system must also be done for each ply. The plies can then be treated as multiple parallel paths similar to an electrical circuit with multiple parallel resistive paths to find the total thermal properties for the laminate.

5.3.1 1D Thermal Sidewall Analysis: Lamina Ply Orientation

From Conley, the expressions for thermal conductivity of a lamina, in three orthogonal directions (one direct. parallel to the fibers and other two directs. perpendicular to the fibers) are:

$$k_{11} = V_f * k_{f11} + (1 - V_f) * k_m \qquad (5)$$

and

$$k_{22} = k_m * \frac{k_{f22} * (1 + V_f) + k_m * V_m}{k_{f22} * V_m + k_m * (1 + V_f)} \qquad (6)$$

$$k_{33} = k_{22} \qquad (7)$$

Where, k_{11} = lamina thermal conductivity, parallel to fibers.

k_{22} & k_{33} = lamina thermal conductivity, perpendicular to fibers and each other.

(Cont.) k_{f11} = fiber thermal conductivity, in the fiber longitudinal direction.

k_{f22} = fiber thermal conductivity, in the fiber transverse direction.

k_m = thermal conductivity of the resin matrix.

V_f = Volume fraction of fiber.

V_m = Volume fraction of matrix.

The orientation of the fibers in each lamina ply is then rotationally translated back to the original coordinate system. The rotation is done by multiplying the mathematical matrix of thermal values for the ply by the cosine or sine of the angle that the fibers in the ply are rotated from the original coordinate system. Figures 6 and 7 show how the thermal conductivity decreases or increases in the in-plane directions as the angle of fiber orientation increases from 0^o to 90^o. By referencing the thermal properties of every ply to one coordinate system, the values for each ply can then be combined to get the thermal properties for the entire sidewall laminate.

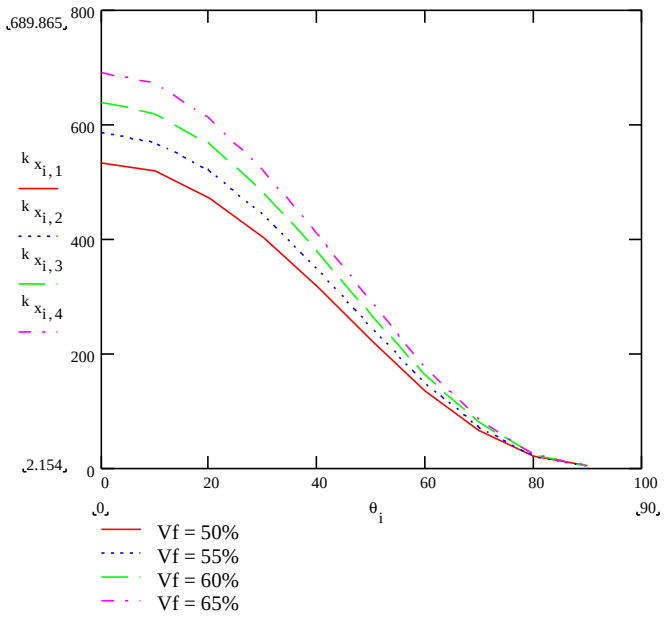

Figure 6: Thermal Conductivity in Reference Coordinate System X-direction versus Ply Angle for a Single Lamina Ply and Varying Fiber Volume Fraction.

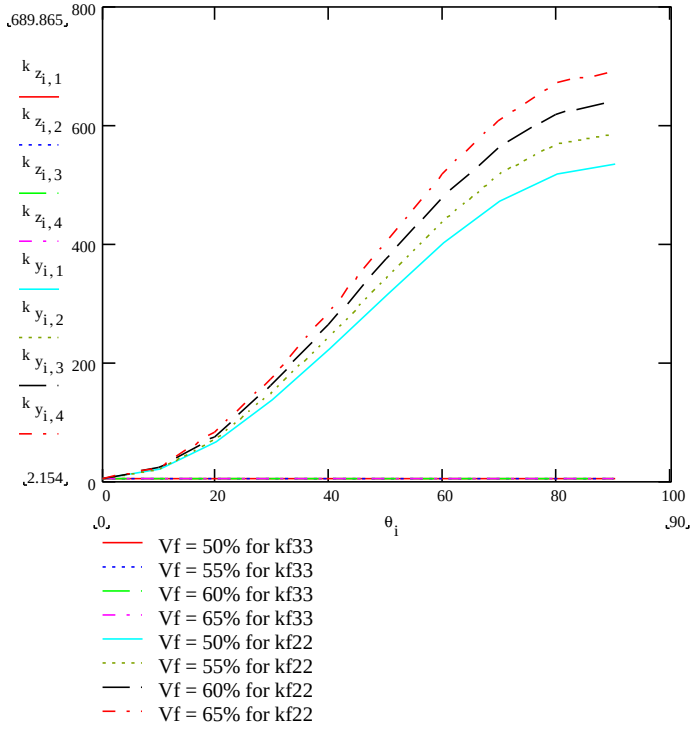

Figure 7: Thermal Conductivity in Reference Coordinate System Y & Z-directions versus Ply Angle for a Single Lamina Ply and Varying Fiber Volume Fraction.

5.3.2 2D Thermal Sidewall Analysis: Laminate Fiber/Ply Stack-up

Originally, several different ply angle combinations were tried in a FE model to determine the thermal conductivity effect. Figure 8 shows the average ΔT from top to bottom of a sidewall as ply angles are changed.

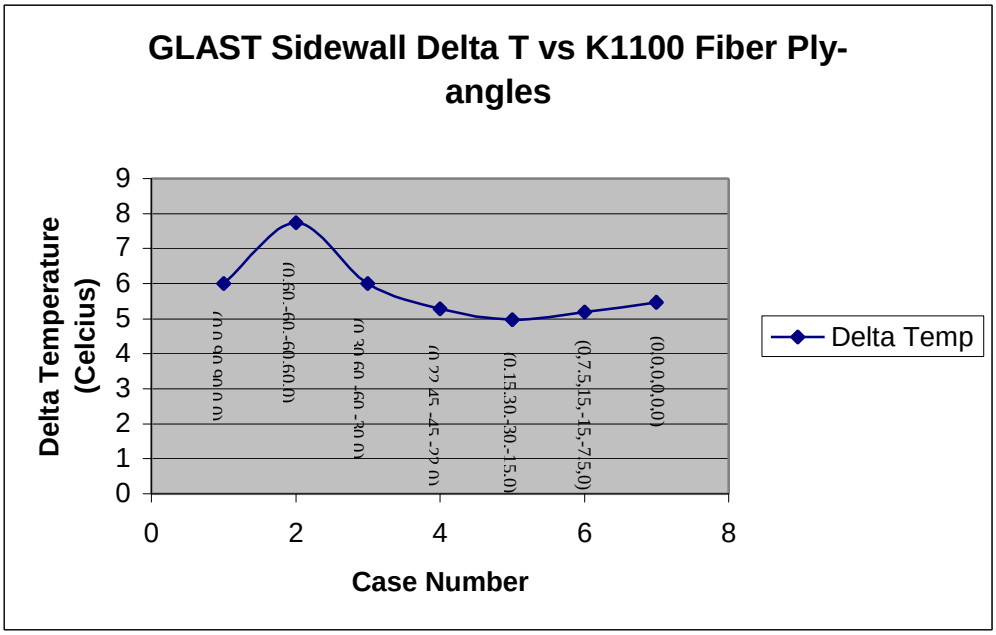

Figure 8. Average ΔT of K1100 Sidewall for Different Ply Angle Combinations.

Case four, although not the optimum was the most practical from a composites fabrication standpoint. The ply angles in case four are common for composite industry standards. The ΔT for the sidewall in case four is also slightly better than case seven for a unidirectional composite panel. The difference is associated with better thermal cross distribution along the width of the panel, making the effective area of heat transfer much larger than with straight unidirectional plies.

The method used above for determining ply-angle orientation for the sidewall was very cumbersome and quite time consuming. To get a better distribution of how ΔT varies with ply-angle orientation, a program was written that would automatically vary ply-angles in a FE model and plot the resulting ΔT as a surface map. Figure 9 shows one of the surface plots generated for a K1100 fiber GFRP sidewall.

The surface plot has the same characteristic shape as figure 8, but it easily shows more of the contour of the trough that forms around a ply-angle of 15 degrees and the expected peak for both plies having their orientation normal to the direction of thermal conduction in the panel. The surface plot was generated by first considering a six-ply laminate since that is the minimum number of plies needed to form a quasi-isotropic composite. Since the six-ply laminate is symmetric, only three ply-angles need to be specified. One of the plies is always orientated in the 0^o ply direction, leaving the other two ply-angles (α & β) to be specified. The other two plies are

defined from 0^o to 90^o by setting one ply-angle (α) and then running multiple cases with the other ply-angle (β) being incremented from 0^o to 90^o.

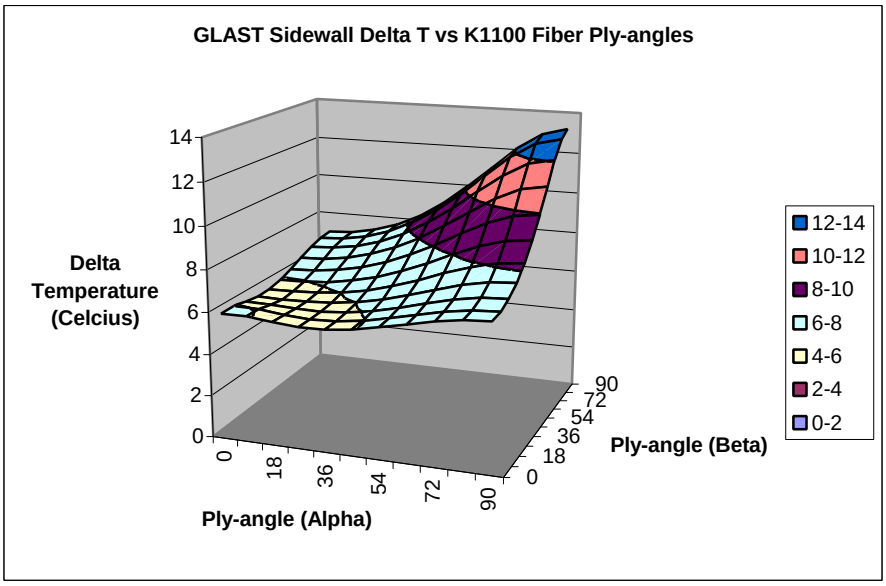

Figure 9. Sidewall Delta T versus K1100 Fiber Ply-angles.

Multiple surface plots were run with varying thermal conductivities for the different fiber possibilities. In addition to K1100 fibers, P30 and YS-90A fibers were studied. 3D FE sidewall analysis for the tower was done next to define thermal sharing between the four sidewalls.

5.3.3 3D Thermal Sidewall Analysis: Tracker Tower

Thermal load sharing will occur between sidewall panels for each tracker tower. This is due to the large number of thermal pathways between sidewalls in the tray closeouts and facesheets. A brief FE analysis was done to determine how much thermal load sharing would occur in the GLAST tracker towers. Figure 10 shows the thermal gradients across four sidewalls connected at the corners.

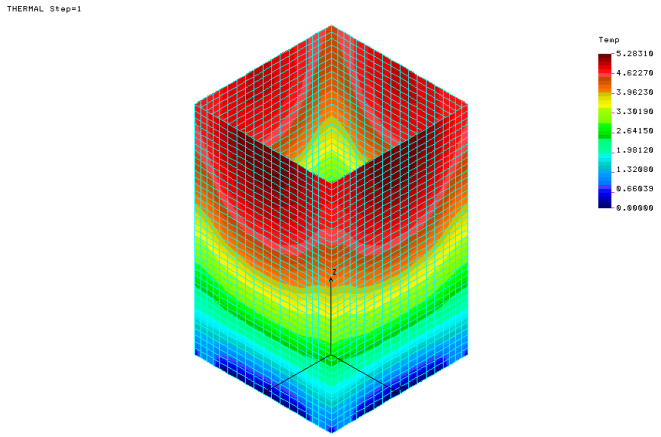

Figure 10: K1100 fibers, ply angle sequence: (0, +/-22.5, +/-45|$_{symmetric}$)

The thermal gradients are relatively even around the four sidewalls. The maximum gradient from the top of the sidewalls to the bottom is 5.28°C. The model was revised to include the facesheet material between the four sidewalls. Figure 11 shows the resulting thermal gradients.

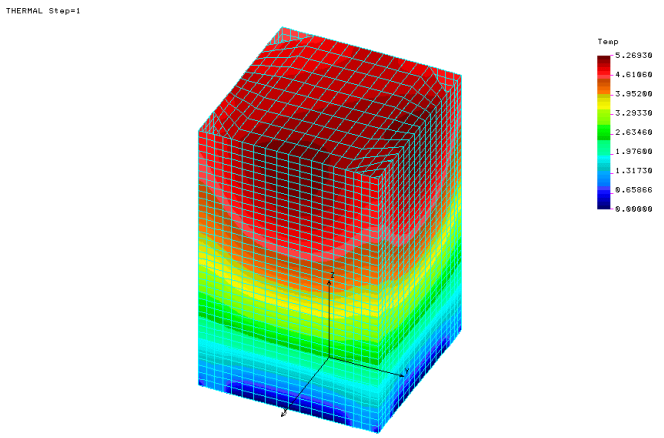

Figure 11: K1100 fibers, ply angle sequence: (0, +/-22.5, +/-45|$_{symmetric}$)

With YSH50/RS-3 facesheet material included in the FE model, the maximum thermal gradient changed to 5.27°C. The thermal gradient changed by 0.01°C indicating a minimal redistribution of thermal load through the facesheets. This is probably due to the high thermal conductivity of the K1100 fibers in the sidewalls versus the minimal cross sectional area of the facesheets, which are 152µm to 229µm thick depending on the type of tray.

Since the sidewalls are actually connected to the tray closeouts in the corners and not to each other, any redistribution of thermal load will occur through the tray closeouts. Selection of material for the closeouts will determine how much thermal load is transferred between the sidewalls. Once the tray closeouts are fully designed, another analysis determining the thermal gradients of the sidewalls with the tray closeouts should be performed.

5.4 Thermal Deformation Considerations for Sidewall Material

For thermal loads, a material's thermal expansion governs alignment, geometric stability and thermally induced stresses. Higher coefficient of thermal expansion (CTE) materials will experience greater deformations for a given temperature change. As tray alignment and overall geometric stability are requisite for the tracker design, low-CTE materials are preferable. Thermal stresses for components and/or fasteners may also be an issue if non-matched CTE materials are used. Figure 3 (above) gives a summary of CTE values for potential sidewall materials.

5.4.1 Tracker tray alignment issues

Tray (detector) alignment is especially critical for the GLAST tracker. Thermal loading of the tracker towers will vary from the center of the tracker to the outer walls. We predict that the sidewalls will dominate tower deformations under thermal loading. Figure 12 shows a potential deformation mode for a single tower under a side-to-side temperature differential. We can reasonably assume that such a differential is linearly distributed. For an isotropic material, the curvature of the tower sidewalls is given by

$$k = -\frac{a\Delta T}{h} \qquad (3)$$

where h it the tower width in the x-direction. Small angle approximation then gives the tower top rotation $q = kL$ where L is the tower height. For point P, displacements in the x- and z-direction are $-\frac{1}{2}qL$ and $a\Delta TL$, respectively. Point Q will move an additional $\frac{1}{2}a\Delta Th$ in the x-direction[†]. A summary of predicted displacements for the two indicated points on the tower is given in Table 5-1.

Finite element analyses were also conducted to verify that the sidewalls dominate the deformation under thermal loads. Displacement results for aluminum sidewalls and tray closeouts, under a side-to-side temperature differential of 2°C, are given in the Appendix.

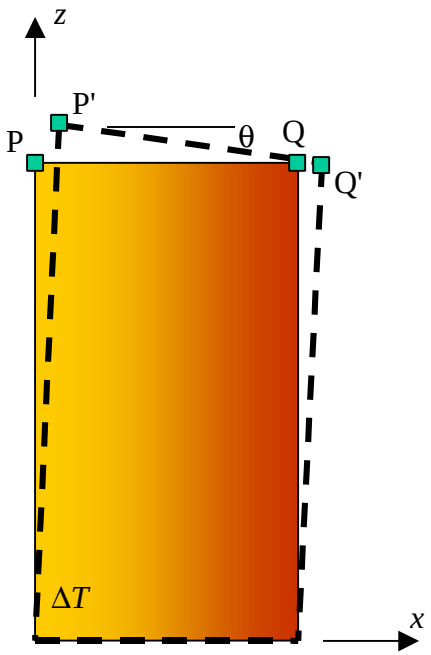

Figure 12: Deformed shape of tower under side-to-side temperature differential.

[†] We consider only the horizontal displacement of point Q. Assuming $T = 0$ at x = h, point Q has negligible vertical displacement. For composites, horizontal displacements of Q depend upon the material's x-direction CTE.

		D*T* = 2°C [*x*=0 ? *T*=2; *x*=*h* ? *T*=0]			D*T* = 5°C [*x*=0 ? *T*=5; *x*=*h* ? *T*=0]		
Material	**CTE (ppm/°C)**	**P'$_x$ (mm)**	**P'$_z$ (mm)**	**Q'$_x$ (mm)**	**P'$_x$ (mm)**	**P'$_z$ (mm)**	**Q'$_x$ (mm)**
Aluminum	23.6	23.1	29.3	32.4	57.7	73.2	80.9
Beryllium	11.3	11.1	14.0	15.5	27.6	35.0	38.7
Gr-CE Composite	*z*: -1.5 *x*: -0.5	-1.5	-1.9	-1.8	-3.7	-4.7	-4.4
CC Composite	*z*: -1.5 *x*: -1.2	-1.5	-1.9	-2.2	-3.7	-4.7	-5.5

Table 5-1: Tracker tower top displacements for side-to-side temperature differential.

5.4.2 CTE material mismatch

CTE mismatches in adjacent materials will induce stress due to unequal expansion (and/or contraction) of the materials under temperature changes. Therefore, matching CTE values (or minimizing CTE mismatch) for the tray closeouts[†] and sidewall materials should be considered. The current design for the tray closeout incorporates small spacer posts, machined at each of the four corners[‡]. Additionally, small fasteners will be used to attach the sidewalls to each tracker tray. Figure 13 shows a corner of a typical tray closeout.

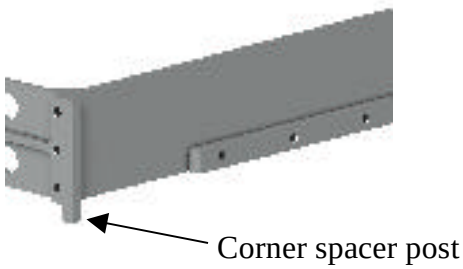

Figure 13: Spacer post and fastener locations at corner of typical tray closeout.

The closeout corner spacer post is restricted in size by spatial constraints of the tracker. Its dimensions are approximately 3.5 x 3.5mm (for a cross-sectional area of 12.25mm^2). If CTE

[†] Tray closeouts are the frames which surround each tray, providing support for the tracker detectors, conversion layers and other hardware.
[‡] Machined spacer posts may be replaced by (captured) spacer blocks.

mismatches exist between the closeout and sidewall materials, then each corner post must counter forces imposed by two sidewalls as the tower undergoes a temperature change from the assembly temperature.

We assume that there are sufficient fasteners along the length of towers to consider a continuous sidewall-to-closeout connection. For a conservative first-order analysis, we assume that the sidewalls act as axial (*Z*-direction) members. The average internal force, *P*, due to a temperature change in two continuously connected materials is given by

$$P = (a_S - a_C)\Delta T \frac{A_S E_S A_C E_C}{A_S E_S + A_C E_C} \qquad (4)$$

where *S* and *C* refer to the sidewall and closeout, respectively. Stresses in the corner posts are determined in the usual manner. Table 5-2 shows resultant forces and stresses for the corner post for CTE-mismatched materials under a modest ±20°C temperature change. Tests have shown that the compressive strength of two-dimensional CC composites ranges from 63 to 75MPa[2] depending on fiber orientation. Therefore, CC closeouts would probably not work with aluminum or beryllium sidewalls.

For design purposes, we should assume conservatively that the internal force P will be developed fully in shear at the outermost fasteners connecting the sidewalls to the closeouts (i.e., those at the top and bottom of the tower). Spatial constraints require that the screws be limited in size to approximately 1-2.5mm in diameter. The loads shown in Table 5-2 indicate that substantial local stresses could be developed at the fastener locations. Additionally, if we assume a conservative static friction value of 1.0, we can see that the required normal loads to resist slippage could be excessive.

Sidewall Material	Closeout Material	Resultant Internal Force [N]	Corner post stress [MPa]
Aluminum	Beryllium	877	71.6
Aluminum	Carbon composite	1435	117.1
Beryllium	Aluminum	208	17.0
Beryllium	Carbon composite	775	63.3
Carbon composite	Aluminum	424	34.6
Carbon composite	Beryllium	975	79.6

Table 5-2: From assembly D*T* = ± 20°C – resultant forces and corner post stress for CTE mismatch in sidewall and closeout materials.

5.5 Stiffness and Mass Considerations

A common measure for material structural performance is the material's S/W ratio. Generally, the higher a S/W ratio is, the more it is suited for space applications. Of the materials shown in Figure 4, beryllium and carbon composites have the highest S/W values. Thus, for achieving minimized SI mass for a given stiffness requirement, these materials should be considered as the best potential candidates. Further mechanical design issues will be discussed in additional documents.

5.6 Radiation Length Considerations

In general, it is considered that higher radiation length (RL) materials are better suited for the tracker structural components. Radiation length is based on the average distance, L_R, over which a high-energy electron (E_e +/- > or = to 1GeV) loses all but 1/e (37%) of its energy to Bremsstrahlung.[3] As particles interact with the materials of the tracker they can mimic the signal events that are trying to be measured in the silicon fields, thus making it difficult to determine momentum and direction of an incoming gamma ray as it passes through the tracker. Opacity to gamma rays is greater for higher RL materials. Low RL materials will induce an increased number of background events, which are difficult to disseminate from signal events, and are therefore less desirable. Figure 5 shows RL for the various materials under consideration for tracker structural components. From this figure, we can assess that beryllium or carbon composites are the best candidates.

5.7 Summary of Candidate Materials for Tracker Sidewalls

A summary of the candidate materials is given in Table 5-3. From the previous analyses and comparisons, we can now rate each of the materials. CTE mismatch problems are omitted from this summary, except to note that CTE matched materials are highly recommended for the tray closeouts and the tracker sidewalls.

5.7.1 Additional Comments on Thermal Conductivity

Of the candidate materials, carbon composites (both CC and Gr-Ep) have the highest potential thermal conductivities. *High-end* composite laminates can be used to attain conductivity of up to approximately 450W/mK. Because conductivity is principally a function of fiber orientation, composites can be designed with directional conductivity in mind. Lower cost composite laminates will yield conductivity values similar to that of beryllium. Beryllium and aluminum both have isotropic thermal conductivities.

For the purposes of initial mechanical and thermal testing, both P30 C-C and YS90A CE materials have been chosen for prototype sidewalls. Total thickness of each laminate panel is 1.5mm. The panel lay-up for each is $0^o/90^o$ fabric, 0^o, -22.5^o, 22.5^o, 45^o, 90^o, -45^o|symmetric.

Candidate Material	Thermal Conductivity	Radiation Length	Stiffness/ Weight	CTE Alignment Performance	Relative Material Cost	Relative Machining Cost[1]
Aluminum	Fair	Poor	Fair	Poor	Low	Low
Beryllium	Good	Excellent	Excellent	Fair	Very High	Very High
Carbon-carbon	Good to Excellent	Good	Excellent	Excellent	High to Very High	Moderate to high
Graphite-Epoxy	Good to Excellent	Good	Excellent	Excellent	High to Very High	Moderate to high

[1]Notes:

Aluminum – Al-alloys are easily machined.

Beryllium – Be dust is toxic which necessitates higher machining costs.

Carbon-carbon – CC machines easily. Care must be taken to remove carbon dust after machining.

Graphite-Epoxy – Gr-Ep machines readily (requires diamond tooling). Fiber dust must be removed.

Table 5-3: Summary table for comparison of candidate tracker sidewall materials.

5.7.2 Comments on Costs

Aluminum will no doubt be the lowest cost material of the candidates. However, the RL of aluminum is significantly higher than beryllium or the carbon composites. Aluminum is also slightly higher in density. Sheet beryllium although the best candidate as far as RL is concerned would cost significantly more (possibly $3500 for each sidewall) than the other material candidates. Additionally, machining costs for beryllium can be quite expensive due to the carcenogic nature of the machined dust.

Both of the carbon composites have the best potential for the sidewall material. The RL is almost as high as beryllium and the weight is less than aluminum. From a cost standpoint, the GFRP panels are expected to be lower in price than the P30 carbon due to the large volume of processing involved with P30 carbon during fabrication. Both should be much less than the cost of beryllium.

6. References

1. Keating, S., E. Swensen, E. Ponslet and S. Ney, "Tracker Design Requirements for GLAST," Hytec Technical Note HTN-102050-0021, May 8, 2001.
2. Ponslet, E., F. Biehl and E. Romero, "Carbon-Carbon Composite Closeout Frames for Space Qualified, Stable, High Thermal Conductivity Detector Support Structures," Hytec Technical Note HTN-102021-0001, May 2000.
3. Miller, W.O., Gamble, M., Thompson, T. and Ziock H., "Superconducting Super Collider Silicon Tracking Subsystem Research and Development", LA-12029, December 1990.

7. Appendix

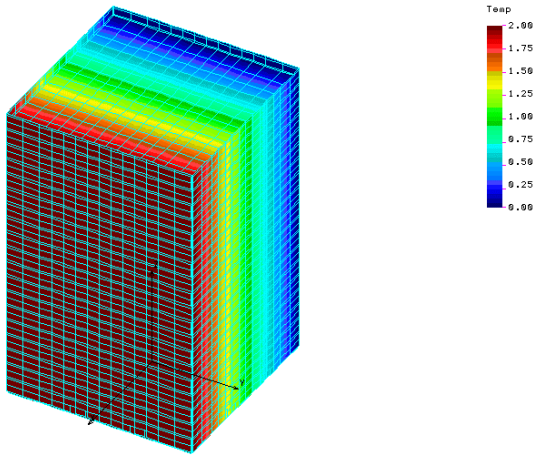

Figure A6: Assumed tracker tower temperature distribution for a side-to-side D*T* of 2°C.

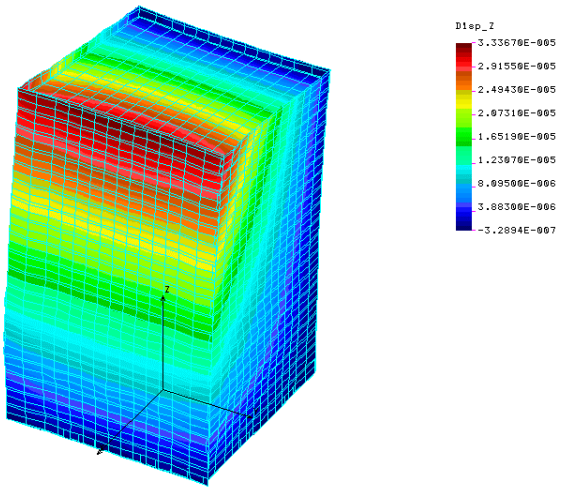

Figure A7: Finite element model of tracker tower showing *x*-direction displacements. Tower top displacements are similar to those from the simplified analysis.

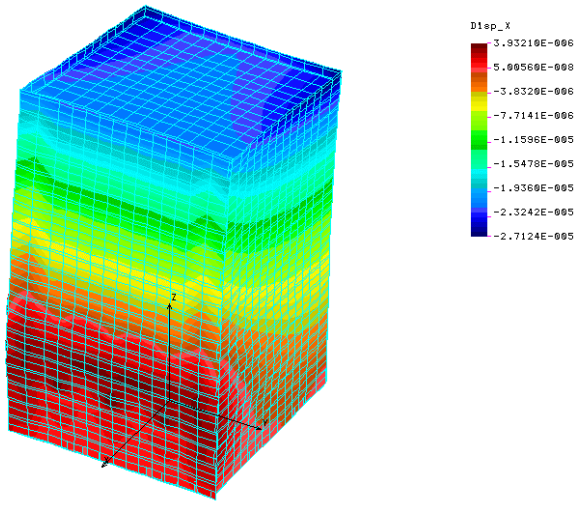

Figure A8: Finite element model of tracker tower showing *x*-direction displacements. Tower top displacements are similar to those from the simplified analysis.